Observation of Scaling in the Dynamics of a Strongly Quenched Quantum Gas

E. Nicklas,[1] M. Karl,[1] M. Höfer,[1] A. Johnson,[2] W. Muessel,[1] H. Strobel,[1] J. Tomkovič,[1] T. Gasenzer,[1] and M. K. Oberthaler[1]

[1]*Kirchhoff-Institut für Physik, Ruprecht-Karls-Universität Heidelberg, Im Neuenheimer Feld 227, 69120 Heidelberg, Germany*

[2]*Laboratoire Charles-Fabry, Institut d'Optique Avenue Augustin Fresnel, 91 127 Palaiseau Cedex, France*

(Received 17 September 2015; published 11 December 2015)

We report on the experimental observation of scaling in the time evolution following a sudden quench into the vicinity of a quantum critical point. The experimental system, a two-component Bose gas with coherent exchange between the constituents, allows for the necessary high level of control of parameters as well as the access to time-resolved spatial correlation functions. The theoretical analysis reveals that when quenching the system close to the critical point, the energy introduced by the quench leads to a short-time evolution exhibiting crossover reminiscent of the finite-temperature critical properties in the system's universality class. Observing the time evolution after a quench represents a paradigm shift in accessing and probing experimentally universal properties close to a quantum critical point and allows in a new way benchmarking of quantum many-body theory with experiments.

DOI: 10.1103/PhysRevLett.115.245301 PACS numbers: 67.85.-d, 03.75.Kk, 05.30.Jp, 05.30.Rt

Scaling laws and symmetries are at the foundations of modern science. They allow us to put phenomena as different as opalescent water under high pressure, protein diffusion in cell membranes [1], and early-universe inflationary dynamics [2,3] on the same structural footings. Typically, scaling is observed in thermal equilibrium or in relaxation dynamics close to equilibrium [4–9], while recently the scaling hypothesis has been extended to far-from-equilibrium dynamics [7,10–12].

For spatially extended systems, it is natural to ask how its different parts are correlated with each other. Close to critical configurations, the essential physics is typically captured by a single parameter ε measuring the distance to criticality, and a universal function. Generalizing this to nonequilibrium quantum dynamics implies that the universal function explicitly includes time evolution. For example, given a time-dependent characteristic length scale ξ, scaling implies a self-similarity relation

$$\xi(s^{-\nu z}t; s\varepsilon) = s^{-\nu}\xi(t;\varepsilon), \tag{1}$$

with positive scaling factor s and critical exponents ν, z. This relation reflects that the spatial structure for fixed system parameter ε at a given time is the same as the structure at different ε, at suitably rescaled times.

Our experiments reveal such scaling behavior in a rubidium condensate in a quasi-one-dimensional configuration. The atoms are in two hyperfine states, which we denote as $|\uparrow\rangle = |F = 2, m_F = -1\rangle$ and $|\downarrow\rangle = |F = 1, m_F = 1\rangle$. The collisional interaction between atoms in these states is tuned by use of an interspecies Feshbach resonance [13,14] such that the system is in the immiscible regime; i.e., the two components tend to minimize their overlap [Fig. 1(a)]. Specifically, the interspecies scattering length $a_{\uparrow\downarrow}$ is chosen larger than the intraspecies scattering lengths $a_{\uparrow\uparrow}$ and $a_{\downarrow\downarrow}$. In the experiment, we chose $\alpha = a_{\uparrow\downarrow}/\sqrt{a_{\uparrow\uparrow}a_{\downarrow\downarrow}} \approx 1.23$. Demixing of such kind has already been observed experimentally [15–17], and studied theoretically [18–23]. Varying the strength of linear Rabi coupling between the two atomic species allows tuning across a quantum phase transition between the immiscible and miscible regimes.

Here, we study the dynamics after a sudden change, i.e., quench, of the linear coupling, observing the time evolution of the spatially resolved density patterns of the two components $n_\uparrow(y)$ and $n_\downarrow(y)$ along the extended axis of the trap, on either side of the miscible-immiscible transition [Fig. 1(b)]. Because of the repulsive interactions between the individual components, the local atomic density $\rho(y) = n_\uparrow(y) + n_\downarrow(y)$ is to a very good approximation constant, such that only the density difference $n_\uparrow(y) - n_\downarrow(y)$ fluctuates. Consequently, the gas can be considered as a homogeneously distributed, coupled collective spin ensemble, characterized by a continuous angular-momentum field $\mathbf{J}(y)$ [Fig. 2(a)]. The longitudinal extension of $\sim$200 μm allows us to explore the miscible regime where the expected length scales are of the order of a few microns, as well as the immiscible side, with expected domain sizes of a few tens of microns. The z component $J_z(y) = [n_\uparrow(y) - n_\downarrow(y)]/\rho(y)$ of the "Schwinger spin" normalized to the total density is related to the density difference, and spin correlations $G_{zz}(y, y', t) = \langle J_z(y)J_z(y')\rangle_t$ between different points y, y' can be determined from the density patterns [Fig. 1(b)].

The long-wavelength dynamics of our spin fluid is given, to a good approximation [24], by a translationally invariant nonlinear XXX-type Heisenberg Hamiltonian density [37],

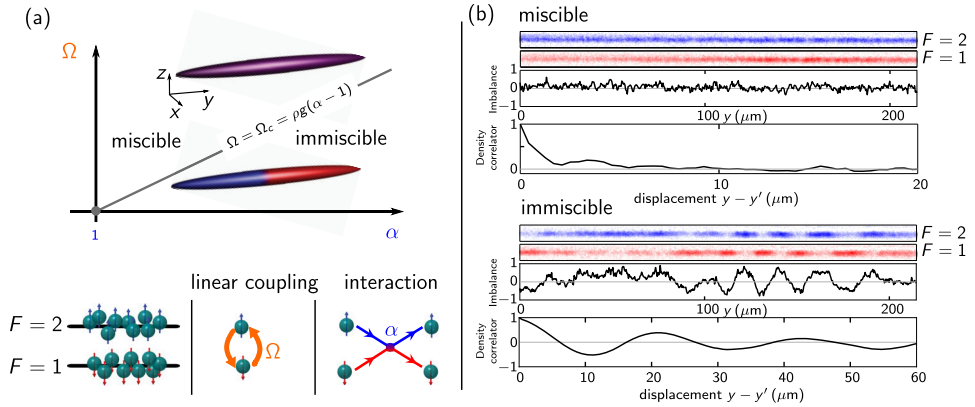

FIG. 1 (color online). Details of the experimental system. (a) Phase diagram, distinguishing miscible and immiscible phases of the elongated degenerate Bose gas of rubidium atoms in $F = 2$ (blue) and $F = 1$ (red) hyperfine states. The state of the system is controlled by linear coupling of the levels, with Rabi frequency Ω, and by tuning the collisional interaction between atoms in the hyperfine states, quantified by the relative strength $\alpha = a_{\uparrow\downarrow}/\sqrt{a_{\uparrow\uparrow}a_{\downarrow\downarrow}}$ of inter- and intraspecies scattering lengths (experimentally fixed to $\alpha \approx 1.23$). A quantum phase transition occurs at $\Omega_c = \rho g(\alpha - 1)$, with 1D atom density ρ and intraspecies coupling constant g. (b) The system is initially prepared far in the miscible regime, and then Ω quenched close to Ω_c. After different evolution times the two species are absorption imaged. Snapshots of the patterns emerging on either side of the transition are shown, with corresponding normalized density imbalance $[n_\uparrow(y) - n_\downarrow(y)]/\rho$ and density correlation functions between spatially separated points y and y'. The correlations on the miscible side exhibit decay on a characteristic length scale, while oscillations on the immiscible side reflect domain formation as seen in the density.

$$\mathcal{H} = [|\partial_y \mathbf{J}|^2/4 + \Omega J_x - \Omega_c J_z^2/2]\rho/2. \tag{2}$$

The first term represents the Heisenberg spin coupling. The term ΩJ_x provides the local coupling of the two components, in analogy to an effective magnetic field acting transversely to the spin J_z, with strength given by the Rabi frequency Ω of the linear coupling. In addition, a "single-ion anisotropy" [38] term J_z^2 appears, which results from the local collisional interaction between the two components, with $\Omega_c = \rho g(\alpha - 1)$ proportional to the tunable interaction strength between the spins. As the scattering lengths of the respective rubidium hyperfine scattering channels are very close, we take $a_{\uparrow\uparrow} = a_{\downarrow\downarrow} = g/(\hbar\omega_\perp)$, such that $\alpha = \hbar\omega_\perp a_{\uparrow\downarrow}/g$. This system reveals, at zero temperature, a quantum phase transition at $\Omega = \Omega_c$, where the Rabi-induced mixing of the components cancels the effect of the interspecies scattering, with the order parameter given by the magnetization $\langle J_z \rangle$. Specifically, for a strong effective magnetic field $\Omega > \Omega_c$ the spins in the ground state are polarized in the x direction; i.e., the two components cannot spatially separate although the bare system ($\Omega = 0$) is phase separating. This is confirmed experimentally [Fig. 1(b)].

A generic scaling hypothesis which includes dynamics out of equilibrium implies that the spin-spin correlations $\langle J_z(y) J_z(y') \rangle_{t,\varepsilon} = G_{zz}(y - y', t; \varepsilon)$ after a sudden quench of the linear coupling obey

$$G_{zz}(s^{-\nu} y, s^{-\nu z} t; s\varepsilon) = s^{-\nu-\eta} G_{zz}(y, t; \varepsilon), \tag{3}$$

where $\varepsilon = \Omega/\Omega_c - 1$ is determined by the final effective magnetic field Ω after the quench. ν and z are critical exponents, and η is known as anomalous exponent. In the experiment we reach this out-of-equilibrium regime by initially preparing the system with a fast $\pi/2$ microwave radio frequency pulse in a J_x spin state, which is the ground state of the system in the infinite-linear-coupling limit ($\Omega \gg \Omega_c$). Then, the intensity of the radio frequency field is quickly reduced, switching ε to its final value. Adjusting the linear coupling during the following evolution compensates for the change of Ω_c due to the loss of particles, which was independently determined.

The correlations $G_{zz}(y, t; \varepsilon)$ developing on the miscible side ($\varepsilon > 0$) are shown in Fig. 2(b), in comparison with homogeneous Bogoliubov–de Gennes theory predictions [39], averaged over the density inhomogeneity in the trap and convoluted with the optical point spread function of the imaging system. Fitting an exponential to the short-distance falloff of the observed correlation functions, we extract a correlation length $\xi(t; \varepsilon)$ which shows near-linear growth after the initial quench [Fig. 2(c)]. The Bogoliubov prediction (solid lines) qualitatively reproduces this rise as well as the oscillations seen for larger ε. The damping of the oscillations seen at smaller ε is attributed to effects of the transverse trapping potential.

We extract the maximum correlation length for different ε within the first 12 ms after the quench, where this observable is still weakly affected by the atom loss. Using the theoretically expected exponent of 0.5 for rescaling the correlation functions at a fixed time ($t = 12$ ms) they all fall on a universal curve [Fig. 3(a),

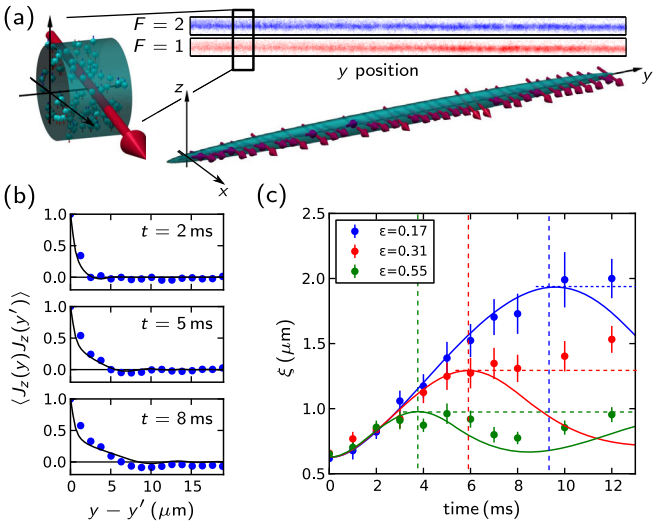

FIG. 2 (color online). Time evolution of correlations after quench to the miscible side of the quantum phase transition. (a) Two-component gas as a coupled collective spin ensemble. The spatially resolved density difference between $F = 1$ and $F = 2$ allows the extraction of the local z component of the collective spin vector $\mathbf{J}(y)$. (b) Measured spin correlation function $G_{zz}(y, y', t) = \langle J_z(y) J_z(y') \rangle_t$ at three different times after a quench to $\varepsilon = \Omega/\Omega_c - 1 = 0.17$, showing buildup of spatial correlations. Solid black lines show Bogoliubov–de Gennes mean-field predictions. (c) Time evolution of the correlation length $\xi(t;\varepsilon)$, for three different ε, deduced by fitting an exponential to the short-distance falloff of the extracted correlation data. The Bogoliubov evolution (solid lines) recovers the initial near-linear rise of ξ, with slope given by the speed of (spin-wave) sound, and captures the maximum correlation length at a characteristic time depending on ε. The predicted oscillatory behavior is experimentally observed for larger ε, while the maximum correlation length reached at short times is robustly detected in all cases. Dashed lines serve as a guide to the eye, marking the predicted first maxima. For the scaling analysis of the data, the correlation lengths are compared at a fixed time; see Fig. 3.

upper panels]. Extracting characteristic length scales as indicated, we find scaling according to Eq. (1) [lower panels of Fig. 3(a)]. The exponent extracted from a linear fit of ξ on a double-log scale is $\nu = 0.51 \pm 0.06$ [Fig. 3(a), lower right-hand panel]. The scaling exponent is robust with respect to varying the range of the exponential fit of the correlation functions and the way of extracting a characteristic length after the initial linear rise. In the immiscible regime, $\varepsilon < 0$, we choose the domain size L_d and find an exponent of $\nu = 0.51 \pm 0.04$ [Fig. 3(a), lower left-hand panel]. As a result, in both the miscible and immiscible regimes, we find self-similarity under rescaling $y \to \varepsilon^{\nu} y$ with $\nu = 1/2$, with correlations following different universal functions.

To obtain the dynamical exponent z we analyze the observed time dependence of the correlation functions, focusing on the point of time τ where $\xi(t)$ levels off after the initial linear rise [Fig. 3(b), upper panel]. For this, we determine the crossing point of two independent linear fits to the short- and long-time behavior. The resulting dependence of $\tau(\varepsilon)$ is compared on a double-log scale to a power law with exponent $\nu z = 1/2$ [Fig. 3(b), lower panel, dashed line]. The deviation of our data from this power law for large ε can be understood within Bogoliubov theory, which predicts $\xi(t;\varepsilon) = (2m\Omega_c\varepsilon)^{-1/2} |\sin(\Delta(\varepsilon)t)|$ [24]. The time $t_{1,\varepsilon}$ of the first maximum [solid line in Fig. 3(b), lower panel], related to the characteristic time τ, is inversely proportional to the gap, i.e., zero-momentum-mode frequency $\Delta(\varepsilon) = \Omega_c \sqrt{\varepsilon(\varepsilon + 1)}$.

On either side of $\varepsilon = 0$, the critical exponents extracted from our data are consistent with Bogoliubov–de Gennes mean-field predictions. To reveal the limitations of mean-field theory and study the effects due to the excitation of total-density fluctuations, we have performed semiclassical simulations of coupled Gross-Pitaevskii equations for the two components (Fig. 4). We define a correlation length ξ_0 in terms of the zero-momentum limit of the Fourier transform of the spin-spin autocorrelation function, $G_{zz}(k,t;\varepsilon) = \int dy \exp\{-iky\} G_{zz}(y,t;\varepsilon)$ [24]. For $\varepsilon > 0.1$, we find very good agreement of the computed correlation length at the first maximum (blue points) with mean-field scaling (solid black line). The numerical data show that, for $\varepsilon \lesssim 0.05$, the extracted correlation length scale at the first maximum deviates from a simple mean-field power law and saturates to a finite value at vanishing ε. This ε dependence of ξ_0 shows universal crossover behavior reminiscent of an equilibrium one-dimensional Ising system [40]. The spontaneous breaking of the discrete Z_2 symmetry under $J_z \to -J_z$ allows for spin-$\uparrow/\downarrow$ domain formation, and, thus, according to the standard theory of critical phenomena, the transition in our system belongs to the Ising universality class [41]. The analysis of the numerically observed crossover behavior requires a discussion of nonperturbative corrections to the experimentally observed mean-field scaling. As seen in Fig. 4, our current experiment touches on the regime where nonperturbative corrections start to become important.

In conclusion, we have demonstrated the possibility of probing universal properties close to a quantum critical point by quenching the system out of equilibrium and observing the short-time evolution long before equilibration. With that, our experiment opens a new path to study universal properties building on phase coherence in closed many-body systems. This is essential for benchmarking quantum many-body theory, moving towards a quantum simulator of universal critical phenomena.

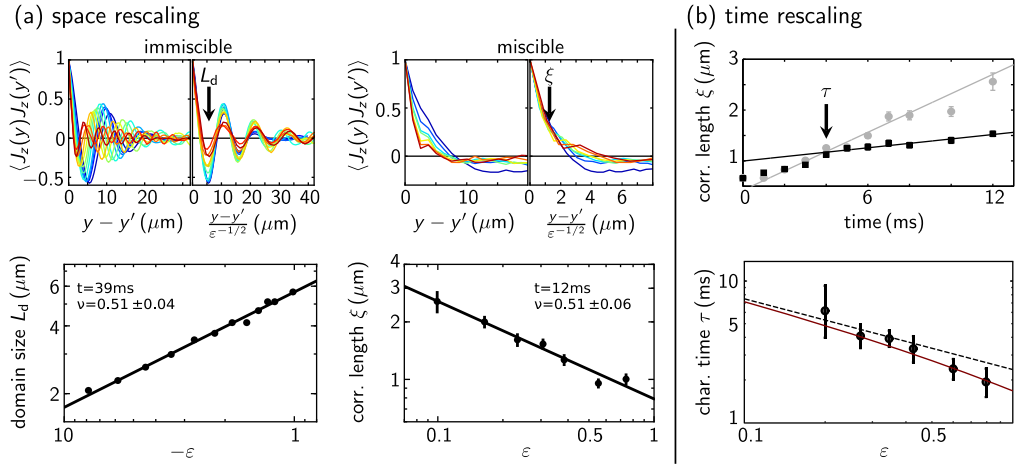

FIG. 3 (color online). Spatial and temporal scaling of the spin-spin correlations. (a) Spatial correlations after quenches to different proximities ε from the critical point (color coded), on the immiscible (left-hand panels, at $t = 39$ ms) and miscible side (right-hand side, $t = 12$ ms). Top panels: The correlation functions, under a rescaling $y \to y\varepsilon^{\nu}$ of the distance dependence with mean-field exponent $\nu = 1/2$, fall on a universal curve. Bottom panels: ε dependence (double-log scale) of the characteristic length scales deduced from the correlation functions. The straight lines reveal values for the critical exponent $\nu = 0.51(4)$ on the immiscible and $\nu = 0.51(6)$ on the miscible side of the transition. (b) Temporal scaling of the spin-spin correlations. The characteristic time τ for different ε is obtained as the intersection point of the linear fits to the initial rise of $\xi(t)$ (gray symbols for $\varepsilon = 0.1$) and to the behavior after ξ deviates from this rise. The procedure of determining the intersection is exemplarily shown in the upper panel for $\varepsilon = 0.23$. In the lower panel we compare the extracted $\tau(\varepsilon)$ to a mean-field scaling with $\nu z = 1/2$ (dashed line) and to the Bogoliubov prediction $\tau \sim 1/\Delta$, with gap $\Delta(\varepsilon) = \Omega_c\sqrt{\varepsilon(\varepsilon+1)}$, also applicable at larger $\varepsilon \gtrsim 1$ (solid line).

The project was initiated in extensive discussions with Jacopo Sabbatini and Matthew Davis in the context of the Kibble-Zurek mechanism in 1D spin systems. We acknowledge the important input from Isabelle Bouchoule on the Bogoliubov description of the observations, and thank Tilman Zibold for support on the experiment. We thank J. Berges, S. Erne, F. Essler, and J. M. Pawlowski for discussions. This work was supported by Deutsche Forschungsgemeinschaft (GA677/7,8), Heidelberg University (CQD), the Helmholtz Association (HA216/EMMI), and the EU (FET-Proactive grant AQuS, Project No. 640800).

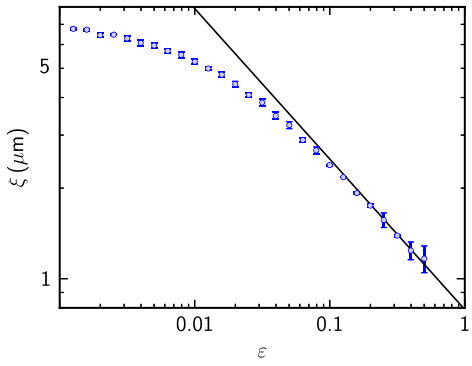

FIG. 4 (color online). Scaling analysis at short times after the quench. Correlation length $\xi_0(t;\varepsilon)$ on the miscible side of the transition, at the time of the first maximum of ξ_0 after the quench. The solid black line marks the Bogoliubov prediction $\xi_{\mathrm{Bog}} = \sqrt{\hbar/(2m\Omega_c\varepsilon)}$ also shown in Fig. 3(a). Closer to the critical point, the open colored symbols show results of semiclassical simulations of the quench dynamics. In the experimental range ($\varepsilon \gtrsim 0.1$), simulation data and Bogoliubov mean-field prediction agree. For $\varepsilon \lesssim 0.1$, the simulations demonstrate a deviation from the mean-field power law and saturation for $\varepsilon \to 0$.

[1] S. L. Veatch, O. Soubias, S. L. Keller, and K. Gawrisch, Proc. Natl. Acad. Sci. U.S.A. **104**, 17650 (2007).
[2] G. Hinshaw *et al.*, Astrophys. J. Suppl. Ser. **208**, 19 (2013).
[3] P. Ade *et al.*, Astron. Astrophys. **571**, A16 (2014).
[4] P. Coleman and A. J. Schofield, Nature (London) **433**, 226 (2005).
[5] T. Donner, S. Ritter, T. Bourdel, A. Öttl, M. Köhl, and T. Esslinger, Science **315**, 1556 (2007).
[6] X. Zhang, C.-L. Hung, S.-K. Tung, and C. Chin, Science **335**, 1070 (2012).
[7] S. Braun *et al.*, Proc. Natl. Acad. Sci. U.S.A. **112**, 3641 (2015).
[8] N. Navon, A. L. Gaunt, R. P. Smith, and Z. Hadzibabic, Science **347**, 167 (2015).
[9] R. Landig, F. Brennecke, R. Mottl, T. Donner, and T. Esslinger, Nat. Commun. **6**, 7046 (2015).
[10] A. Lamacraft, Phys. Rev. Lett. **98**, 160404 (2007).
[11] D. Rossini, A. Silva, G. Mussardo, and G. E. Santoro, Phys. Rev. Lett. **102**, 127204 (2009).
[12] E. G. Dalla Torre, E. Demler, and A. Polkovnikov, Phys. Rev. Lett. **110**, 090404 (2013).
[13] A. Widera, O. Mandel, M. Greiner, S. Kreim, T. W. Hänsch, and I. Bloch, Phys. Rev. Lett. **92**, 160406 (2004).

[14] M. Erhard, H. Schmaljohann, J. Kronjäger, K. Bongs, and K. Sengstock, Phys. Rev. A **69**, 032705 (2004).
[15] L. E. Sadler, J. M. Higbie, S. R. Leslie, M. Vengalattore, and D. M. Stamper-Kurn, Nature (London) **443**, 312 (2006).
[16] J. Kronjäger, C. Becker, P. Soltan-Panahi, K. Bongs, and K. Sengstock, Phys. Rev. Lett. **105**, 090402 (2010).
[17] E. Nicklas, H. Strobel, T. Zibold, C. Gross, B. A. Malomed, P. G. Kevrekidis, and M. K. Oberthaler, Phys. Rev. Lett. **107**, 193001 (2011).
[18] E. Timmermans, Phys. Rev. Lett. **81**, 5718 (1998).
[19] D. H. Santamore and E. Timmermans, Eur. phys. Lett. **97**, 36009 (2012).
[20] J. Sabbatini, W. H. Zurek, and M. J. Davis, Phys. Rev. Lett. **107**, 230402 (2011).
[21] J. Sabbatini, W. H. Zurek, and M. J. Davis, New J. Phys. **14**, 095030 (2012).
[22] S. De, D. L. Campbell, R. M. Price, A. Putra, B. M. Anderson, and I. B. Spielman, Phys. Rev. A **89**, 033631 (2014).
[23] M. Karl, B. Nowak, and T. Gasenzer, Sci. Rep. **3**, 2394 (2013).
[24] See Supplemental Material at http://link.aps.org/supplemental/10.1103/PhysRevLett.115.245301, which includes Refs. [25–36], for a detailed discussion of the experimental methods and further details on the theory.
[25] J. W. Weyssenhoff, Nature (London) **157**, 766 (1946).
[26] K. Kasamatsu, M. Tsubota, and M. Ueda, Phys. Rev. A **71**, 043611 (2005).
[27] *Quantum Magnetism*, edited by U. Schollwöck, J. Richter, D. J. J. Farnell, and R. F. Bishop, Lecture Notes in Physics Vol. 645 (Springer, Berlin, 2004).
[28] E. D. Siggia and A. E. Ruckenstein, Phys. Rev. Lett. **44**, 1423 (1980).
[29] K. Kasamatsu and M. Tsubota, Phys. Rev. A **74**, 013617 (2006).
[30] A. M. J. Schakel, *Boulevard of Broken Symmetries—Effective Field Theories of Condensed Matter* (World Scientific, Singapore, 2008).
[31] A. Altland and B. Simons, *Condensed Matter Field Theory*, 2nd ed. (Cambridge University Press, Cambridge, England, 2010).
[32] C. Lee, Phys. Rev. Lett. **102**, 070401 (2009).
[33] A. A. Nersesyan, A. Luther, and F. V. Kusmartsev, Phys. Lett. A **176**, 363 (1993).
[34] P. C. Hohenberg and B. I. Halperin, Rev. Mod. Phys. **49**, 435 (1977).
[35] P. B. Blakie, A. S. Bradley, M. J. Davis, R. J. Ballagh, and C. W. Gardiner, Adv. Phys. **57**, 363 (2008).
[36] A. Polkovnikov, Ann. Phys. (Amsterdam) **325**, 1790 (2010).
[37] J. Zinn-Justin, *Quantum Field Theory and Critical Phenomena* (Clarendon Press, Oxford, 2002).
[38] H.-J. Mikeska and A. K. Kolezhuk, in *Quantum Magnetism*, edited by U. Schollwöck, J. Richter, D. J. J. Farnell, and R. F. Bishop, Lecture Notes in Physics Vol. 645 (Springer, Berlin, 2004), p. 1.
[39] P. Tommasini, E. J. V. de Passos, A. F. R. de Toledo Piza, M. S. Hussein, and E. Timmermans, Phys. Rev. A **67**, 023606 (2003).
[40] S. Sachdev, Nucl. Phys. **B464**, 576 (1996).
[41] F. Zhan, J. Sabbatini, M. J. Davis, and I. P. McCulloch, Phys. Rev. A **90**, 023630 (2014).